

UDC 551.5

FOEHN EFFECT DIAGNOSIS WITH WATER VAPOR SATELLITE IMAGERY

Fedoseeva N.V., Kokorina D.A.

*Russian State Hydrometeorological University, Saint-Petersburg,
e-mail: kokorinadasha2000@gmail.com*

The wind foehn is a complex meteorological phenomenon. It occurs as a result of the downward movement or sliding of air along the slope of the mountains. This strong, dry and hot wind is found in almost all mountainous regions of our planet and has a negative impact on the environment. In this work, based on the data of daily satellite imagery obtained by the MODIS spectroradiometer, 20 cases of foehn were analyzed for the period from 2019 to 2022 in European mountain systems. The attribution of foehn types was carried out according to H. Neumeister's classification. The analysis of multispectral images showed that in the images in the water vapor bands the region of the foehn is deciphered as a local area of black tone with clear edges on the lee side of the mountain barrier, which makes this type of imagery a unique tool for detecting the foehn in satellite images. The analysis of the characteristics of air masses, performed with the help of the Eumetsat Airmass RGB model, in the cases of each type of foehn, also demonstrated the promise of water vapor imagery.

Keywords: Foehn wind, Airmass RGB model, water vapor satellite imagery, MODIS, Aqua, Terra

A foehn is a warm and dry (sometimes hot) wind blowing from mountain ranges into valleys and foothills [1]. The action of the foehn is associated with the interaction of the general circulation of the atmosphere and the orography of the area, with a peculiar regime of cloudiness and precipitation being most often observed [2, 3].

The wind foehn is widespread throughout the Earth [4, 5]. It affects a several meteorological phenomena [6] and processes observed in mountain systems [7], as well as agriculture, well-being and physical health of people [8, 9].

The aim of the study was to analyze various types of foehn in the mountain systems of Europe using multispectral satellite imagery data. The materials for the study were the data of daily satellite imagery performed by the MODIS spectroradiometer installed on the Aqua satellite platforms [10].

Materials and methods of research

The classification of H. Neumeister was used to determine the different types of foehn. The classification is based on the features of the visual representation of the foehn on multispectral satellite images and includes four main types: free double-sided foehn; free one-way foehn; boundary layer foehn; tropospheric foehn [11].

The search for each case of a foehn of a certain type was carried out using the decoding features of the cloud field.

To validate the cases determined from satellite images, a scheme was developed that includes step by step 1) analysis of the satellite

image in the infrared channel (11 μm) and the water vapor channel (7.3 μm); 2) analysis of the surface map of the baric field for various periods in the region of action of the foehn; 3) analysis of wind data in the mountain system, taking into account its relief; 4) analysis of data on the wind field, wind gust values, precipitation, relative humidity and air temperature; 5) analysis of the direction and speed of the wind at different isobaric heights, in order to set the height and strength of the foehn.

The search for foehns was carried out in four mountain systems: the Alps, the Pyrenees, the Carpathians and the Scandinavian mountains. A total of 20 foehn cases were identified from 2019 to 2022, of which 5 free double-sided foehn, 5 free one-way foehn, 4 boundary layer foehn and 6 tropospheric foehn.

Satellite image analysis

Further, the most successful cases of each of the four types of foehn in certain mountain systems of Europe are considered in detail. The images shown were taken by the Aqua satellite. Preliminary studies have shown high information content of the use of images in the absorption band of water vapor in the far IR region of the spectrum [12]. In this regard, in this work, in addition to the traditional visible and IR thermal bands for diagnosis the foehn, water vapor bands were used.

Double-sided free foehn

The true color image (Fig. 1a) shows the absence of clouds over the mountain range.

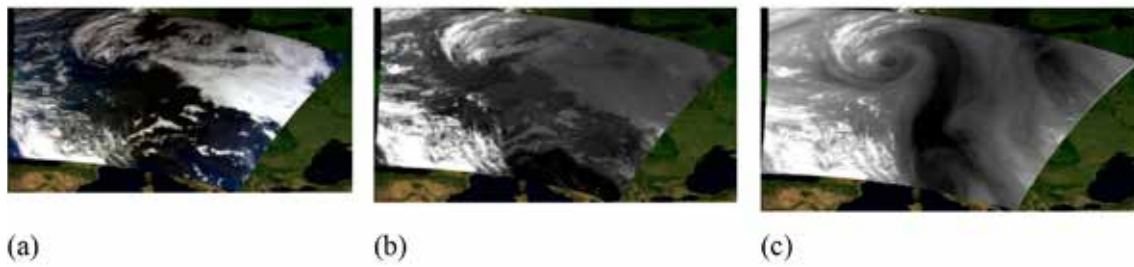


Fig. 1. Satellite image of a two-sided free foehn from 07.11.2020 10:30 UTC according to MODIS / Aqua (a) in true colors, (b) in the thermal IR, (c) in the water vapor band

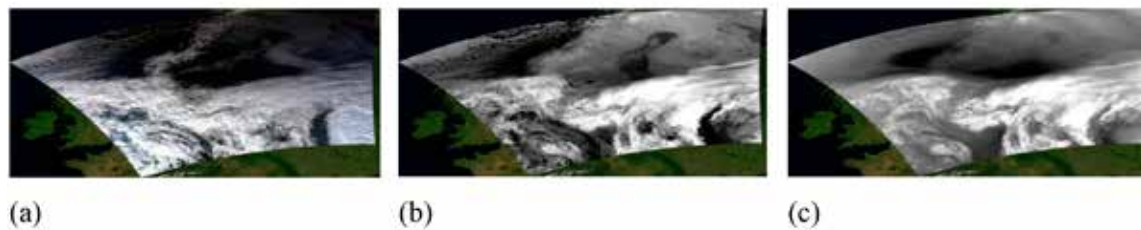


Fig. 2. Satellite image of a free one-sided foehn from 04.11.2019 11:35 UTC according to MODIS / Aqua (a) in natural colors, (b) in IR band, (c) in the water vapor band

As you move away from the ridge, on both sides of the mountain range, in the lower parts of the valleys and foothills, there is fog and haze (only on the south side), deciphered by sharp, repeating the contours of the relief, the edges of cloudiness. This situation is typical for a double-sided free foehn. Analysis of the image in the IR – thermal ($11\ \mu\text{m}$) channel (Fig. 1b) confirmed the presence of fog in the mountain valleys on the northern and southern slopes, which corresponds to grey tone of cloud tops.

The image in the water vapor ($7.3\ \mu\text{m}$) band (Fig. 1c) deciphers a upper level cyclonic atmospheric vortex to the northwest of the mountain range with its center over the North Sea. In addition, the area of dry air corresponding to black tone in the image has a sharp edge, bounded by the crest of the mountain range.

Single sided free foehn

When deciphering an image in the visible range of the electromagnetic spectrum with the case of a one-sided free foehn (Fig. 2a), a cloudless zone with sharp edges is observed on the leeward side of the Scandinavian Mountains, bounded on one side by a mountain range, and on the other side by a field of open convective cells. On the windward side of the mountain range at some distance from it, fog is present in the valley. This situation is a characteristic feature of a loose one-sided foehn.

Analysis of the image in the IR – thermal ($11\ \mu\text{m}$) band (Fig. 2b) confirmed the presence

of fog in the mountain valleys on the windward slope, which corresponds to grey tone of the cloud top.

In the image in the water vapor ($7.3\ \mu\text{m}$) band (Fig. 2c), in the zone of action of the foehn and above the windward side of the mountain range, a region of dry air is deciphered, corresponding to the black tone in the image.

Boundary layer foehn

In the true color satellite image (Fig. 3a), on the windward side of the Carpathian Mountains, an area of stratus cloudiness reaching the crest is observed; on the leeward side, a cloudless area is observed. On the leeward side, wavy clouds, characteristic to this type of foehn, also form. A cyclonic vortex with dense multilayer clouds is observed to the northeast of the mountain range.

Analysis of the image in the IR-thermal ($11\ \mu\text{m}$) range (Fig. 3b) confirmed the presence of layered clouds on the windward and leeward sides with corresponding low brightness pixel and wavy clouds of the middle tier. An occluding low is observed to the northeast of the considered zone.

The image in the water vapor ($7.3\ \mu\text{m}$) channel (Fig. 3c) also deciphers an occluding cyclonic atmospheric vortex to the northeast of the mountain system. In addition, the area of dry air in the area of the foehn, corresponding to the black tone in the image, has a clearly defined edge, limited by the crest of the mountain range.

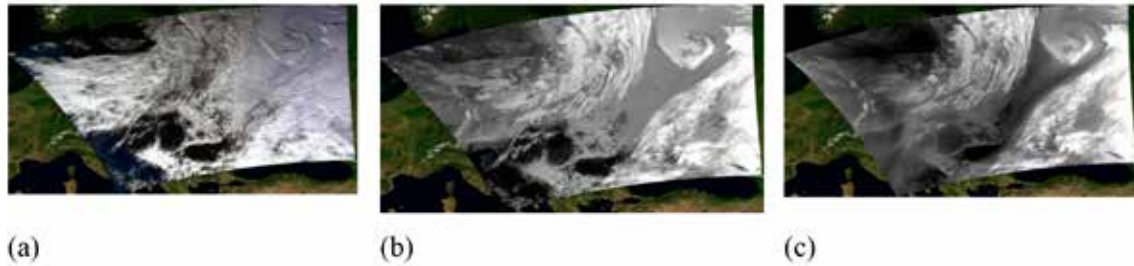


Fig. 3. Satellite image of the boundary layer foehn dated February 8, 2022 11:15 UTC according to MODIS / Aqua data (a) in true color, (b) in IR band, (c) in water vapor band

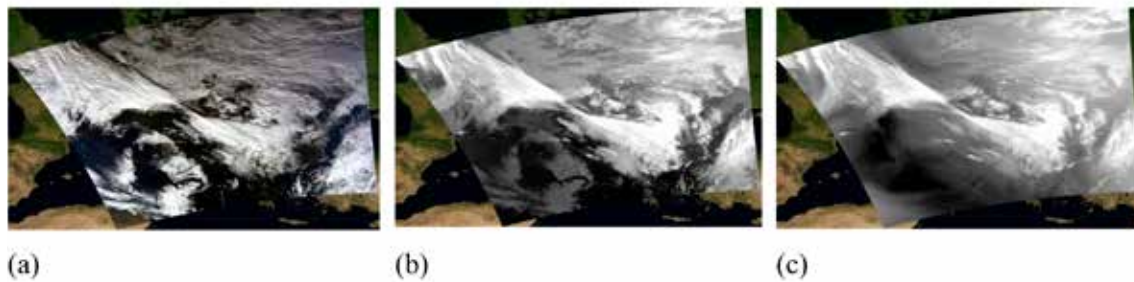


Fig. 4. Satellite image of the tropospheric foehn from January 14, 2021 11:50 UTC according to MODIS/ Aqua data (a) in the visible range of the electromagnetic spectrum, (b) in the infrared range of the electromagnetic spectrum, (c) in the water vapor channel

Tropospheric foehn

Consider the case of a foehn in the Alps on January 14, 2021 at 11:50 UTC. According to the classification proposed by H. Neumeister, the tropospheric foehn in the satellite image should be observed in medium and high mountains.

On the windward side, multi-layer clouds should be observed, reaching the ridge or passing over it. On the leeward side – mostly middle and upper tiers of clouds (0-5 points), wavy clouds may appear. If the foehn does not reach the valleys and foothills, then low stratus clouds or fogs are observed on the leeward side (often in winter).

On the true color satellite image (Fig. 4a), from the windward side of the Alpine Mountains, a cloudy band of a cold front is deciphered, bounded from the south by a mountain range. On the leeward side, there is a cloudless zone with a small area of lee orographic clouds. This distribution of cloudiness is in good agreement with the situation of the tropospheric foehn.

By analyzing the image in the IR – thermal (11 μm) channel (Fig. 4b), we can conclude that in visible image the formation of barrage cloudiness on the windward side of the mountain ridge (a zone of brighter tone compared to the cloudiness of the cold front), is masked of cold front cloudiness corresponding enhancement effect.

The image in the water vapor (7.3 μm) band (Fig. 4c) also clearly shows the obstruc-

tion clouds. In addition, on the leeward side, there is an area of both visible wavy clouds and invisible (in the visible range) mountain waves, a clearly limited area of black tone, corresponding to the dry air zone.

Analysis of images in different ranges of the spectrum made it possible to more accurately determine the types of cloudiness that form when foehn winds occur. It was also found that in the images in the water vapor channel in the foehn effect zone in the middle troposphere, there is an area of dark shades, which indicates a very low content of water vapor in this zone.

Application of RGB model

Also, to confirm that the situation in the image is related to the effect of the foehn wind, an Airmass RGB model was applied, which uses far infrared channels and a water vapor bands [13]. Airmass RGB is a complex but very helpful tool best used for: monitoring Jet streams, PV anomalies, deformation zones and Rapid Cyclogenesis and for discriminating air masses. As an example, discussed above cases for each type of foehn are considered (Fig. 5).

In Airmass RGB images on the leeward side of the mountain range within the black area in 7.3 μm image there is a zone of red color, which, according to color interpretation, corresponds to a dry and high temperature area.

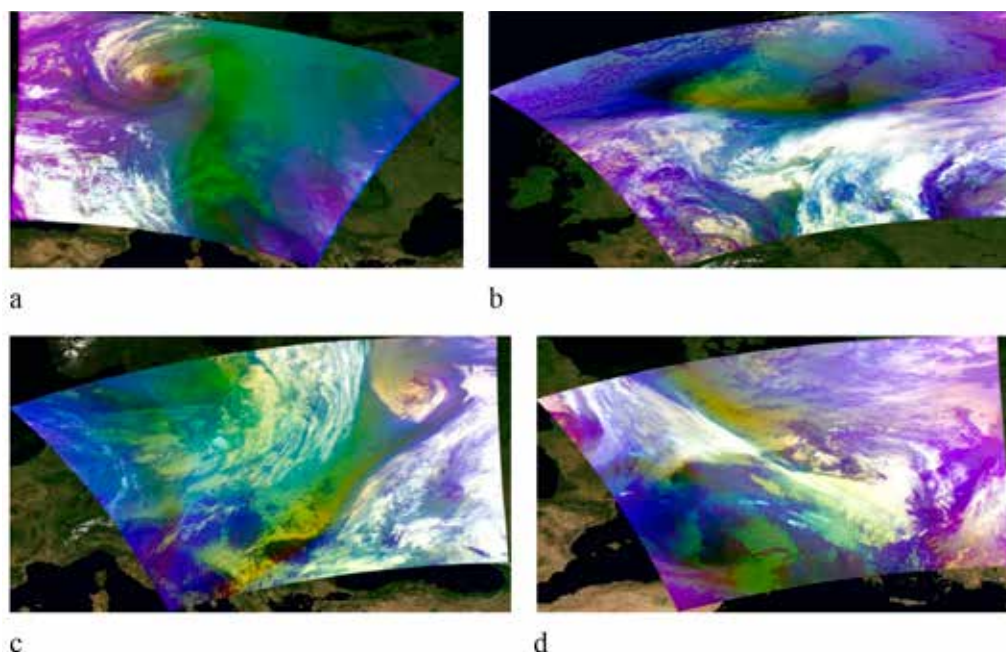


Fig. 5. Satellite images using the RGB color synthesis model
 (a) Alps two-sided free foehn 07.11.2020 10:30 UTC;
 (b) Scandinavian Mountains free one-sided foehn on 11/04/2019 11:35 UTC;
 (c) Carpathians foehn of the boundary layer 02/08/2022 11:15 UTC;
 (d) Alps tropospheric foehn 01/14/2021 11:50 UTC

These shades can be observed over dry desert areas during the summer. In this case, it is obviously to be an area of effect of the foehn. The purple and blue colors in the images above corresponds to a cold air mass, green – to a warm air mass.

Conclusions

In the course of work, various types of foehn were analyzed, taking into account the meteorological conditions, deciphering signs and characteristic types of cloudiness. An analysis of multispectral satellite images showed that, in addition to visual interpretation elements in the visible and IR thermal channels, satellite data in the water vapor channel ($7.3 \mu\text{m}$) can be used to diagnosis of a foehn effect on the leeward side of mountain obstacles. A comprehensive analysis of the obtained images made it possible to demonstrate the reliability of interpretation of various types of foehn wind on satellite images.

References

1. Damiens F. at all. An Adiabatic Foehn Mechanism // *Quarterly Journal of the Royal Meteorological Society*. 2018. Vol. 144 (714). P. 1369-1381.
2. Elvidge, A.D., Renfrew I.A. The causes of foehn warming in the lee of mountains // *Bulletin of the American Meteorological Society*. 2016. Vol. 97. P. 455-466.
3. Whiteman C.D. *Mountain Meteorology: Fundamentals and Applications*. New York: Oxford University Press, 2000. 355 p.
4. Abatzoglou J.T. at all. Global climatology of synoptical-ly-forced downslope winds // *International Journal of Climatology*. 2021. Vol. 41. P. 31-50.
5. Antico L. at all. The foehn wind east of the Andes in a 20-year climate simulation // *Meteorology and Atmospheric Physics*. 2021. Vol. 133. P. 317–330. DOI: 10.1007/s00703-020-00752
6. Li J. at all. A foehn-induced haze front in Beijing: observations and implications // *Atmos. Chem. Phys.* 2020. Vol. 20. P. 15793–15809. DOI: 10.5194/acp-20-15793-2020.
7. Shestakova A.A. at all. The foehn effect during easterly flow over Svalbard // *Atmos. Chem. Phys.* 2022. Vol. 2. P. 1529–1548. DOI: 10.5194/acp-22-1529-2020.
8. Maciejczak A. at all. Impact of Foehn Wind and Related Environmental Variables on the Incidence of Cardiac Events // *International Journal of Environmental Research and Public Health*. 2020. Vol. 17, Is. 8. P. 2638-2653.
9. Mikutta C. A. at all. The Impact of Foehn Wind on Mental Distress among Patients in a Swiss Psychiatric Hospital // *Int. J. Environ. Res. Public Health*. 2022. Vol. 19, Is. 17. P. 10831-10842. DOI: 10.3390/ijerph191710831.
10. Level-1 and Atmosphere Archive & Distribution System Distributed Active Archive Centre LAADS DAAC. URL: <https://ladsweb.modaps.eosdis.nasa.gov/search/> (date of application: 10.02.2023).
11. Ambrozi P., Vel'tishchev N.F., Getts G., Noimaister K.H., Runkanu T., Shabrov V.G. Use of data on mesomassive features of cloudiness in weather analysis. Leningrad: Gidrometeoizdat, 1973. 150 p.
12. Fedoseeva N.V., Efimova Yu.V., Kuroplina V.I. Detection of invisible mountain waves with satellite water vapor imagery // *Proc. Conf. Modern problems of hydrometeorology and sustainable development of the Russian Federation*. 2019. P. 173-174.
13. Airmass RGB | EUMeTrai. URL: <https://www.eumetrain.org/resources/airmass-rgb> (date of application: 10.02.2023).